SUPPLEMENTAL FIGURE LEGENDS

Supplemental Figure 1 PAX3/7 are evolutionarily conserved in *Drosophila*. Shown are amino acid sequence alignment of human PAX3 and PAX7, and the *Drosophila* orthologs Gooseberry (Gsb) and Gooseberry-neuro (Gsb Neuro). For PAX 3/7, only the portion of the protein present in the PAX-FOXO fusion is shown. For Gsb/Gsb-neuro, the sequence of the full-length protein is truncated to correspond to the analogous portion of PAX3/7 present in the fusion. The Paired and Homeodomain DNA binding domains are shown and underlined in bright blue; the octapeptide motif, in green. *Dm = Drosophila melanogaster*; *Hs = Homo sapiens*.

Supplemental Figure 2 Mutation of *Drosophila rols* suppresses PAX7-FOXO1 pathogenicity in vivo. (**A**) The $rols^{P1729}$ allele dominantly suppresses PAX7-FOXO1-mediated lethality. Based on Mendalian ratios, the F_1 adult population should be comprised of 50% control and 50% PAX7-FOXO1-expressing adults (*"Expected"*). PAX7-FOXO1 causes semilethality, as PAX7-FOXO1 adults comprise only 22% of F_1 adults (*"control"*; n = 1127). *Df(3L)vin5* dominantly suppresses PAX-FOXO1 lethality (n = 98), as does the $rols^{P1729}$ allele (n = 101), whereas $rols^{P1027}$ does not (n = 148). (**B**) The $rols^{P1729}$ allele dominantly suppresses PAX7-FOXO1 pathogenicity in larval muscle. At conditions similar to those used in the lethality screen, PAX7-FOXO1 causes scattered muscle fiber atrophy (fibers that either do not develop or persist) and moderate fiber dystrophy/hypotrophy [fibers that develop less fully or incompletely (and as such are noticeably less GFP-fluorescent)]. The orange bars note the representative larval hemisegments shown in the right panels. The orange boxes note equivalent muscle fibers

missing or abnormal in *PAX7-FOXO1* larvae when compared to *wild-type* larvae, and fibers now present and thus rescued in $rols^{P1027}$-suppressed *PAX7-FOXO1* larvae.

Supplemental Figure 3 PAX7-FOXO1-directed misexpression of Rols persists in *Drosophila* gastrulated embryos. (**A**) Whole-mount *wild-type* gastrulated embryos with no detectable PAX-FOXO1 protein expression, and *da>>PAX7-FOXO1* gastrulated embryos with diffuse expression of PAX7-FOXO1 in all germ layers. Original magnification, ×200. (**B**) Whole-mount *wild-type* gastrulated embryos with no detectable Rols protein expression, and *da>>PAX7-FOXO1* gastrulated embryos with diffuse expression of Rols in all germ layers. Original magnification, ×200. (**C**) Posterior poles of embryos in **Panel A**. Original magnification, ×800. (**D**) Posterior poles of embryos in **Panel B**. Original magnification, ×800. α-FOXO1 = anti-FOXO1 immunofluorescence; α-Rols = anti-Rols immunofluorescence; DAPI = DAPI nuclear staining**;** *da>>PAX7-FOXO1* = *daughterless-Gal, UAS-PAX7-FOXO1*; white arrows (**Panels C, D**) = ectodermal cells, yellow arrows (**Panels C, D**) = mesodermal cells, orange arrows = (**Panels B, D**) endodermal cells.

Supplemental Figure 4 mTanc1 mRNA levels decrease as C2C12 myoblasts differentiate. qRT-PCR was used to determine the relative expression levels of mTanc1 mRNA over the six-day course of C2C12 differentiation into syncytial myotubes. Tanc1 levels were normalized to β-actin levels, which does not change during differentiation.

Supplemental Figure 5 PAX3-FOXO1 protein levels in C2C12 myoblasts and RMS-13 cells; PAX7-FOXO1 protein levels in *Drosophila* larvae. (**A**) PAX3-FKHR protein levels in human RMS-13 cells and stable PAX3-FKHR C2C12 cells, compared with human RD cells (a fusion-negative RMS cell line) and control C2C12 cells that do not express PAX3-FOXO1. (**B**) PAX7-FOXO1 protein expression in *Drosophila* (*Dm*) larvae. The arrowhead notes PAX7-FOXO1 protein of the expected size, while the asterisk notes a second band that is either a modified form of PAX7-FOXO1 or a non-specific band.

Supplemental Figure 6 Stably-infected PAX3-FOXO1 C2C12 cells do not fuse and demonstrate consistent PAX3-FOXO1 protein expression levels in the presence of mTanc1 shRNA. (**A**) Crystal violet stain of unfused PAX3-FOXO1-infected C2C12 myoblasts. Original magnification, ×200. (**B**) Tanc1-silencing does not detectably affect PAX3-FOXO1 C2C12 steady-state protein expression levels. PAX3-FOXO1 (~92 kD) protein levels of A6, A10, or A6+A10 treated cells do not detectably differ from control cells 72 hours after transient transfection with the *Tanc1* shRNA constructs. Lysates are from whole-cells, and a non-specific band migrating at ~30 kD serves as the loading control. Lanes were run on the same gel, but were not contiguous.

Supplemental Figure 7 Tanc1 overexpression blocks myoblast fusion potential, but not myogenic differentiation. (**A**) Tanc1-infected C2C12 myoblasts overexpress Tanc1. (**B**) Tanc1 overexpression blocks myoblast fusion but does not alter the terminal differentiation of myoblast into MHC-positive myocytes. Differentiation and fusion indices were calculated as noted previously. (**C**) Crystal violet stain of control C2C12

cells that have fused into syncytial myotubes, and fusion-defective Tanc1-overexpressing cells. Original magnification, ×200. Differentiation and fusion indices were calculated as noted previously; $^{**}P < 0.01$ versus Control.

Supplemental Figure 8 *TANC1* gene silencing rescues PAX3-FOXO1 RMS oncogenicity. (**A**) Decreased expression of TANC1 protein in RMS-13 cells treated with TANC1 shRNA. TANC1 (~202 kD) steady-state protein levels are decreased after transfection of shRNA. Loading control is a non-specific low molecular weight band. (**B**) TANC1-silencing does not detectably affect PAX3-FOXO1 steady-state protein expression levels in RMS-13 cells. PAX3-FOXO1 (~92 kD) protein levels of A6, A10, or A6+A10 treated cells do not detectably differ from control cells after transfection with the *TANC1* shRNA. The asterisk notes a band of smaller molecular weight that is either a non-specific band or a protein-modified form of PAX3-FOXO1. The loading control is a non-specific low molecular weight band. (**C**) Crystal violet stain of round, RMS-13 cells and *TANC1* shRNA-treated cells that exhibit a spindled, myocyte morphology. Original magnification, ×200. (**D**) TANC1 shRNA-treated lines showed a marked decrease in anchorage independent growth and colony formation. Shown is average number of colonies per 20×-lens objective field. **C,D,** Lysates are from whole-cells, collected 72 hours after transient transfection of shRNA. Lanes were run on the same gel, but not contiguous. $^{***}P < 0.001$ versus Control.

SUPPLEMENTAL METHODS

Immunoblotting, immunofluorescence, immunohistochemistry, and software. For the C2C12 and RMS-13 PAX3-FOXO1 and TANC1 immunoblots, cells were harvested 72 hours after transient transfection, and whole-cell lysates generated in RIPA buffer. For the *Drosophila* PAX7-FOXO1 immunoblot, whole-animal lysates of 3rd instar larvae were likewise prepared in RIPA buffer. Primary antibodies used are: mouse monoclonal anti-FOXO1A (1:2000, species reactivity- Human, Sigma-Aldrich, WH0002308M12), rabbit polyclonal anti-TANC1 (1:1000, species reactivity- Human, Sigma-Aldrich, HPA036750). Secondary antibodies (Sigma-Aldrich) were used at 1:5000.

Immunofluorescence staining was performed by fixing cultured cells with 4% paraformaldehyde and 0.1% glutaraldehyde at room temp for 5 min, permeablized and blocked with 0.1% Triton X-100 and 3% BSA in PBS for 15 min. Antibodies used: mouse MF-20 (1:400; Developmental Studies Hybridoma Bank; University of Iowa; Iowa City, IA), Alexa-488 goat anti-mouse (1:5000; Invitrogen). Cells were mounted in vectashield with DAPI (Vector Laboratories). A Ventana Discovery automated immunostainer was used for immunohistochemistries, with standard immunoperoxidase techniques and counterstained with hematoxylin; primary antibody was rabbit TANC1 (1:250; #A303-19A).

Fusion and differentiation indices were calculated from three independent experiments. For each experiment, four random fields were counted. For fusion, the number of nuclei in bi- or multinucleated myotubes were divided by the total number of nuclei scored. For differentiation, the number of nuclei present in MHC-positive cytoplasmic tissue was divided by the total number of nuclei scored.

For *Drosophila* embryo whole-mount immunofluorescence, embryos were treated as described previously (12) (kindly provided by E. Chen; Johns Hopkins; Baltimore, MD.), incubated in primary antibody overnight at 4°C [1:3000 anti-Rols polyclonal sera (12); 1:50 anti-FOXO1 antibody, Cell Signaling, #2880], secondary antibody at room temperature for 2 h. (1:2000, Alexa-568 goat anti-rabbit, Invitrogen), and mounted in vectashield with DAPI. Microscopy was performed with either an LSM150-meta confocal or Zeiss Axioplan2 fluorescent microscope.

Adobe Photoshop was used to improve black/white/RGB levels in a linear fashion.

Soft agar colony assays. Base Agar layer had 0.5% agar (BD Difco Agar Noble) with 20% RPMI-phenol red (Hyclone). RMS-13 cells were transiently transfected (PLko.1 backbone) with shGFP, shTanc1-A6, shTanc1-A10 and shTanc1-A6+A10. Transfected cells were then suspended in 20% RPMI-phenol red + 0.7% agarose (Mercury reagents). Top agarose layer was a final concentration of 0.35%, plated over the set 0.5% base agar. Plates were incubated at 37^0C. Cells were fed with fresh 20% RPMI every other day and colonies were counted 2-3 weeks after transfection. Colonies were stained with 0.005% crystal violet prior to analysis. Replicate plates were scored independently, and four random 20×-lens fields were scored for each plate.

RT-PCR analyses. Expression of PAX3-FOXO1 in stable cell lines was tested by RT-PCR and sequencing with the following primers: Forward- 5'-CAGCCCACATCTATTCCACAAGC-3'; Reverse- 5'-

CCACTAATAGTACTAGCATTTGAG-3'. For qRT-PCR, RNA was isolated from transfected cells with an RNAqueous-Micro RNA extraction kit (Ambion). RNA was treated with DNaseI prior to reverse transcription (RT). RT was performed using 500 ng of total RNA with SuperscriptIII Reverse Transcription (Invitrogen). Quantitative RT-PCR was performed using Brilliant II SYBR green QPCR master mix (Stratagene), with the following primers: mouse-Tanc1 Forward- 5'-TTTGGCGCCTGCCTGGATG-3', mouse-Tanc1 Reverse- 5'-CCCTCAGTGCGCTGTGGACG-3'; human-TANC1 Forward- 5'-GCCGGAGGTAGGGCACAGGA-3'; human-TANC1 Reverse- 5'-CCACCACCGCGCCTCTGTTT-3'; mouse/human-β-actin Forward- 5'-CCTTCTACAATGAGCTGCGTGTGG-3', mouse/human-β-actin Reverse- 5'-ACGACCAGAGGCATACAGGGACAGC-3'. All PCR products were confirmed by sequencing.

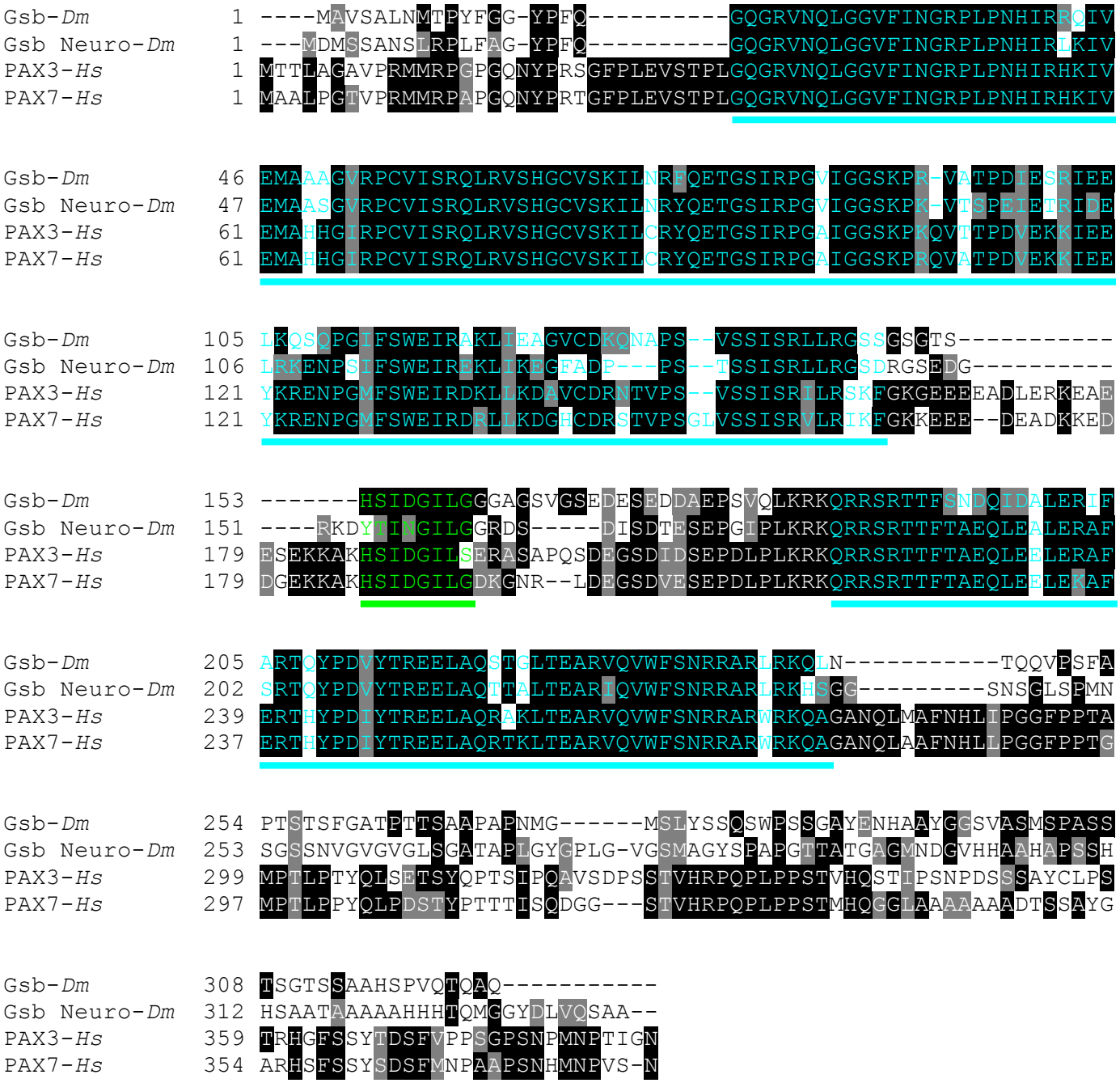

Avirneni-Vadlamudi et al._Supplemental Fig. 1

Avirneni-Vadlamudi et al._Supplemental Fig 2

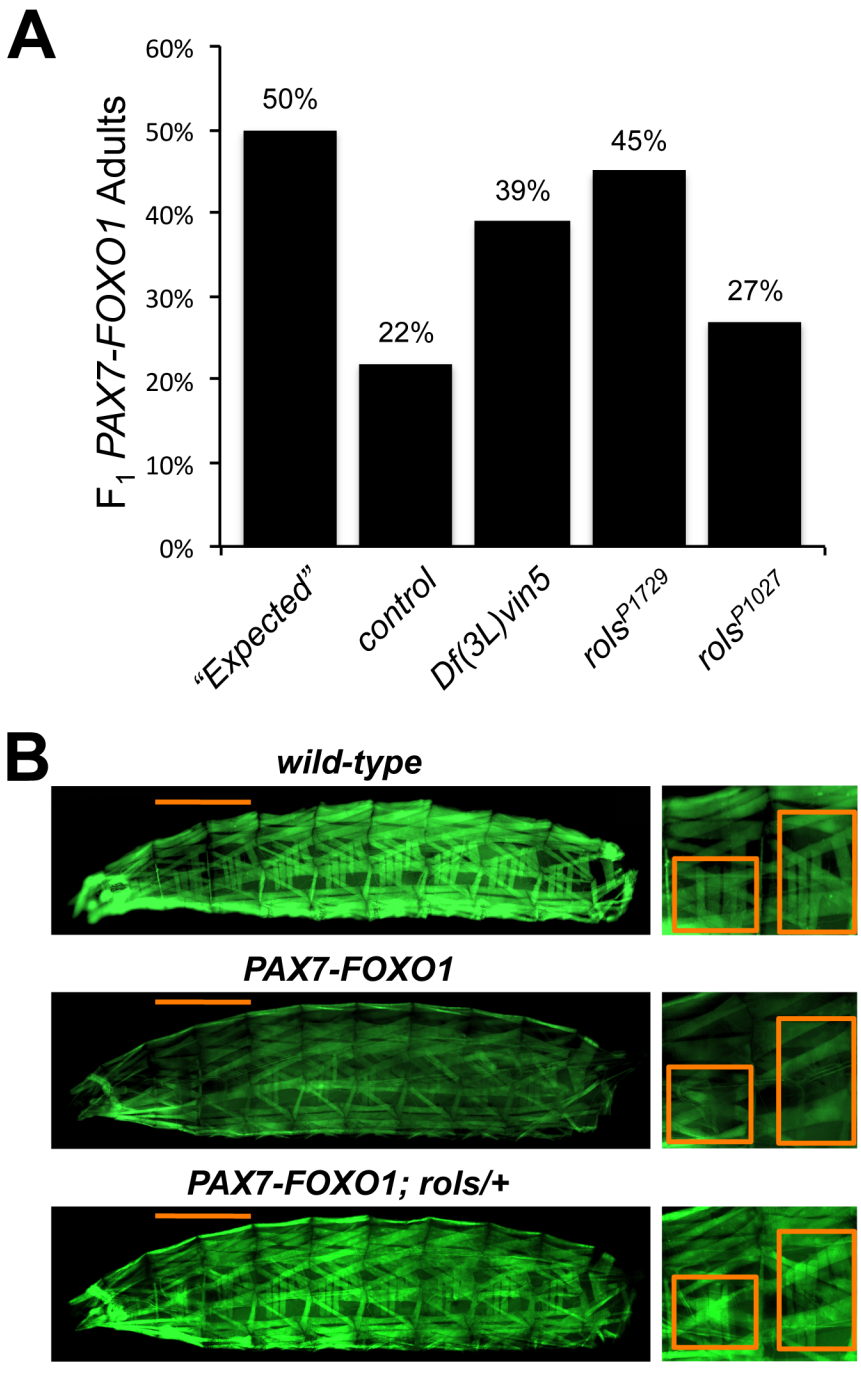

Avirneni-Vadlamudi et al._Supplemental Figure 3

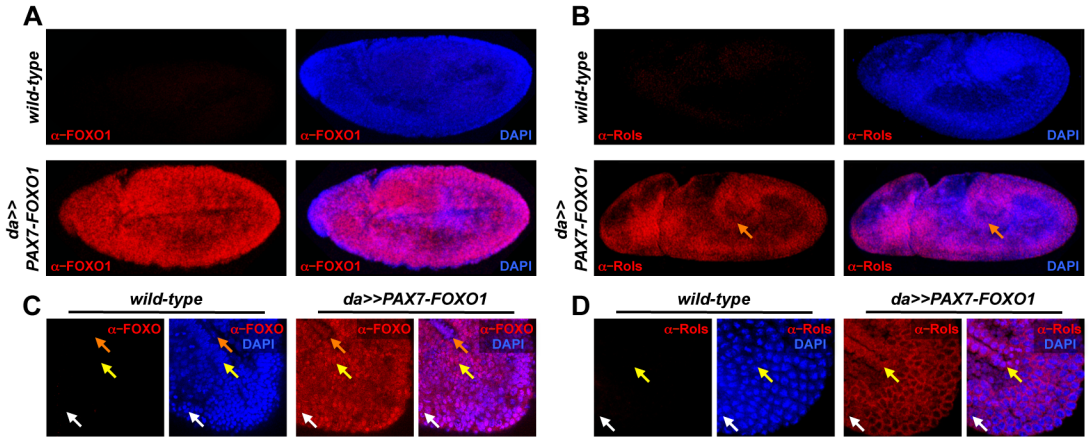

Avirneni-Vadlamudi et al._Supplementary Fig 4

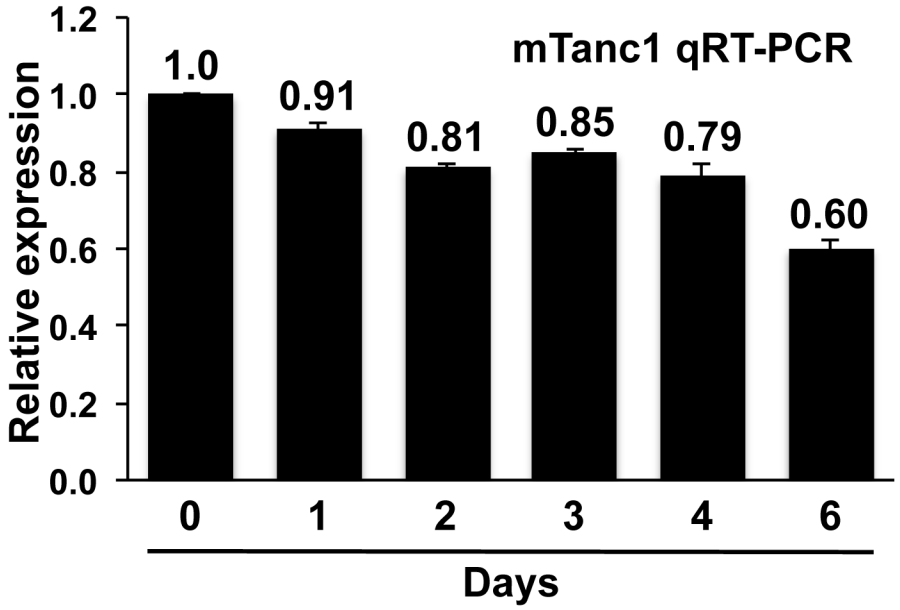

Avirneni-Vadlamudi et al. Supplemental Fig 5

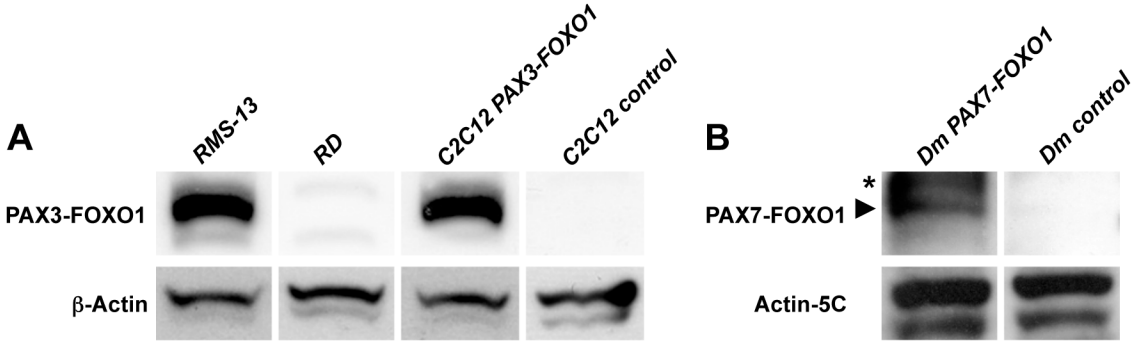

Avirneni-Vadlamudi et al._Supplemental Figure 6

Avirneni-Vadlamudi et al._Supplemental Figure 7

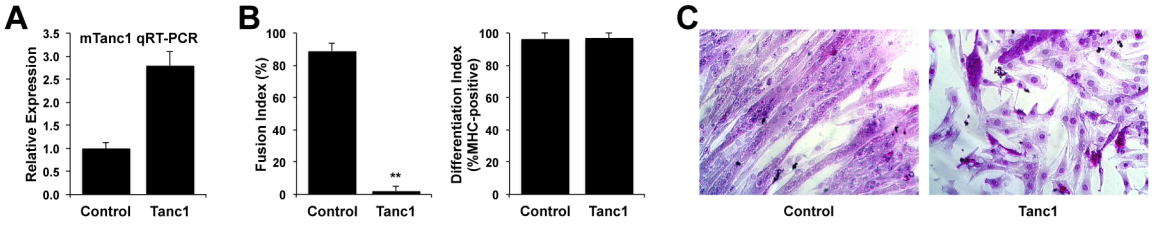

Avirneni-Vadlamudi et al.Supplemental Fig 8